One-Minute Assessment of Photosynthetically Active Radiation (PAR) Models in Uruguay

José Luis Di Laccio[1], Rodrigo Alonso-Suárez[2], Gonzalo Abal[3]

1. Departamento de Física, CeRP del Litoral, Salto, Uruguay
2. Laboratorio de Energía Solar, Facultad de Ingeniería, Universidad de la República, Montevideo Uruguay.
3. Laboratorio de Energía Solar, CENUR Litoral Norte, Universidad de la República, Salto, Uruguay.

Abstract

Photosynthetically Active Radiation (PAR) is the spectral portion of global solar radiation that is primarily relevant to plants' growth processes (between 400 and 700 nm). The PAR fraction (f_p) is the ratio at horizontal surface between the photon's flux per square meter (Q_p) and the global solar irradiance (G_h). In this work, the first assessment in Uruguay of PAR fraction empirical models is presented using 4 years of 1-minute measured data for one site representative of the Pampa Húmeda region. The chosen models have been developed for the 1-hour time scale and use the clearness index and/or the solar altitude as predictive variables. Original and locally adjusted versions of these models are evaluated and compared with the utilization of a constant PAR fraction value (as frequently done in agronomical practice). It is found that polynomial k_t models with original coefficients have acceptable performance, but they cannot be used with locally adjusted coefficients at the 1-minute timescale.

Keywords: PAR radiation, PAR fraction, empirical models, GHI.

1. Introduction

Photosynthetically Active Radiation (PAR) is the portion of solar radiation in the spectral interval 400-700 nm. Part of this radiation is used by plants for photosynthesis and its characterization in a given region is highly relevant for modeling plant growth rates and for proper planning of agricultural production. PAR radiation is measured by specialized sensors as the photon flux (in the 400-700 nm interval) per unit area and expressed as μmol/m^{2}s. On a horizontal surface, this magnitude is denoted by Q_p and it is highly correlated with the global horizontal irradiance, G_h or GHI. If a specialized sensor is not available, Q_p can be indirectly estimated from pyranometer measurements by using an infrared filter which effectively blocks solar irradiance above 700 nm. One of the problems associated with this approach is that, unless an independent UV measurement is available, all UV irradiance below 400 nm will be counted as PAR radiation. For locations for which no PAR measurements are available, Q_p can be estimated from GHI using either a constant PAR fraction or an empirical model, being the latter a lower uncertainty option.

The PAR fraction, which is the quantity of interest in this work, is the ratio $f_p = Q_p / G_h$ expressed in μmol/J. Several previous studies (see for example Tsubo and Walker, 2007) have reported mean PAR fractions between 1.96 and 2.23 μmol/J. Most of these works are based on hourly data from sites in the northern hemisphere. Some authors in the literature work with PAR irradiance (G_p), i.e. the global horizontal irradiance between 400 and 700 nm expressed in W/m^2, either for convenience or for practical reasons (such as indirect measurements). However, Q_p and PAR irradiance are not strictly proportional, since their

ratio depends on the detailed surface solar spectrum at the time and conditions of the measurement. Frequently, this fact is ignored and an approximate conversion constant is calculated from the average incident extraterrestrial solar spectrum. This simple calculation, using the standard ASTM E490 solar spectrum (https://www.astm.org/Standards/E490.htm) normalized to a total solar irradiance of 1361 W/m^2 (Kopp and Lean, 2011) leads to a conversion constant $\kappa = Q_p / G_p$ = 4,566 μmol/J. This value has been used in this work to convert PAR irradiance to photon flux units when referring to published works, with the exception of the work of Tiba and Leal (2007), since these authors explicitly convert the measured photon flux to PAR irradiance using a constant of 4.60 μmol/J.

The focus of this work is the Pampa Húmeda region in southeastern South America, which is climatically and geographically homogeneous and includes parts of Argentina, southern Brazil and the territory of Uruguay. In this region, the percentage of surface area dedicated to agriculture and crop production is among the highest in the world (http://www.fao.org/). For this area, an average PAR fraction of 2.10 μmol/J has been reported in (Grossi Gallegos, 2004) using 26 days of hourly data. Worldwide, most previous work on PAR fraction modelling has been done using hourly or daily data.

As mentioned, the PAR fraction f_p depends on the spectral distribution of solar radiation at ground level, which in turn depends on the state of the atmosphere (precipitable water and aerosol type and content are the main atmospheric factors identified in Alados et al, 1996) and on the air mass or, equivalently, on the Sun's zenith angle (z). Thus, the most relevant variables for PAR fraction modeling are the clearness index ($k_t = G_h / G_0 \cos(z)$, where $G_0 = S \times F_n$ is the solar irradiance incident at the top of the atmosphere, TOA, being S = 1361 W/m^2 the mean total solar irradiance (TSI) and F_n the orbital correction factor) and the solar zenith angle, which can be calculated for each site and time (Iqbal, 1983).

In this work, four pre-existing empirical models for PAR fraction estimation (which use these two variables as descriptors) are evaluated using a quality-controlled 4-year dataset with 1-minute time resolution from a site representative of the Pampa Húmeda region. Sets of good quality simultaneous PAR and GHI measurements are scarce in this region. However, the target region is highly homogeneous with respect to geography and climate. In particular, within the Uruguayan territory the spatial variability of the long-term mean annual solar irradiance (GHI) is below ±5 % of the mean value of 16.9 MJ/m^2 (Alonso-Suárez et al. 2014). Both the original and locally adapted versions of these models are evaluated. The simple approach of considering fp = constant, commonly used by agronomical practitioners, is used as a performance baseline in this work. These models have been chosen for having been developed in a geographical proximity to the region of interest, with the exception of the model by Alados et al. (1996) which was developed using high quality data from Almeria, Spain. A summary of the considered models is shown in Table 1, including their citation, and the location and time-span of the measurements used for their original local training. This is the first work evaluating PAR fraction models in Uruguay and one of the few worldwide on the subject working at the1-minute time scale

This work is organized as follows. Section 2 describes the data being used and its quality assessment, and the models and methodology for their local adjustment and assessment. Section 3 presents the uncertainty evaluation of both original and local adjusted models, and provides recommendations for their utilization in the Pampa Húmeda region. Finally, Section 4 summarizes the main conclusions of this work.

Table 1: Details for the PAR fraction models evaluated in this work. The "type" column refers to whether the PAR photon flux was measured (direct) or estimated from filtered global irradiance measurements (indirect). GG is included as a previous report of the average PAR fraction (constant) for the area of interest. All models considered have been originally developed for the hourly time scale.

Label	Reference	time of measurements	length	type	Location
AL	Alados et al., 1996	1990-1992	2.5 years	direct	Almeria, Spain
TL	Tiba and Leal, 2004	2003-2004	1 year	direct	Recife, Brazil
ES	Escobedo et al., 2006	2001-2005	4 years	indirect	São Paulo, Brazil
TW	Tsubo and Walker, 2007	2000	86 days	direct	South Africa
GG	Grossi et al., 2004	2003	26 days	indirect	San Miguel, Argentina

2. Data and methodology

The measurements used in this work include global horizontal irradiance (G_h or GHI), diffuse horizontal irradiance (G_{dh} or DHI) and Q_p, the PAR photon flux. They were registered between 2016 and 2019 at 1-minute intervals (average of four samples) at the experimental facility of the Solar Energy Laboratory (LES, http://les.edu.uy/) in Salto, Uruguay (latitude = -31.28°, longitude = -57.92° and altitude = 46 m above mean sea level).

The region's climate is classified in the updated Köppen-Geiger classification (Peel et al., 2007) as Cfa (temperate, without dry season and hot summers) with the exception of a small coastal portion dominated by the influence of the Atlantic Ocean, that is classified as Cfb (temperate, without dry season and warm summers). The data used in this work is considered as representative of this broader region.

The G_h and G_{dh} measurements were made with Kipp & Zonen CMP10 pyranometers (spectrally-flat Class A according to the ISO 9060:2018 standard). These pyranometers were mounted on a SOLYS2 Kipp & Zonen solar tracker equipped with CVF4 ventilation and heating units to prevent the accumulation of dust and water droplets on its domes. The SOLYS2 tracker was equipped with a standard shading ball assembly in order to measure G_{dh}, which in this work is only used to strengthen the quality control tests. Both pyranometers have been calibrated every two years against a Kipp & Zonen CMP22 (used as a Secondary Standard pyranometer, Abal et al., 2018) which is kept traceable to the World Radiometric Reference in Davos, Switzerland. The Q_p measurements were made using a Kipp & Zonen PQS1 quantum sensor with factory calibration at the start of the data series.

2.1 Data quality

Quality control of the raw data is of the highest importance when evaluating radiation models. Our quality control procedures are applied in two steps. First, a careful inspection of the dataset is done to remove obvious anomalies (shadows, extreme values, astronomical events such as eclipses, etc.) and diurnal records are selected using the condition $cos(z) > 0$. As a result of this first process, there is a base set of 832108 positive daytime records with the three measurements used here (G_h, G_{dh}, Q_p).

The second step consists of a set of eight quality filters (F1 to F8 in Table 2) which are applied independently to the dataset. These include the relevant BSRN quality procedures (Long and Shi, 2006) for G_h and G_{dh} and also some restrictions on valid Q_p values, as explained below.

F1 selects records with solar altitude > 7° in order to avoid the large uncertainties typical of low-sun conditions. F2 and F3 apply BSRN upper limits with local parameters adequate for the measuring site to GHI and DHI, respectively. F4 filters out points with low clearness index k_t (associated with cloudy conditions) and low diffuse fraction f_d (clear-sky conditions). F5 applies BSRN upper limits to f_d with a tolerance of 5 or 10 % depending on solar altitude. F6 applies an upper limit to the modified clearness index (Perez et al, 1990). F7 applies minimum and maximum limits to the PAR fraction f_p in μmol/J, obtained after inspection of the data.

Table 2: Set of quality control filters applied to the dataset and percentage discarded with respect to the base dataset of 832108 daytime records. The total solar irradiance at TOA is S = 1361 W/m^2.

Filter	Description	Condition	parameters	% discarded
F1	min solar altitude	$cos(z) > cz\ min$	cz min = 0.1219	0.7
F2	upper limit in G_h	$G_h < Go.fcos^a(z) + c$	f = 1.15, a= 1.25, c = 20	0.1
F3	upper limit in G_{dh}	$G_{dh} < Go.fcos^a(z) + c$	f = 1.15, a = 1.25, c = 20	0.0
F4	lower limit for f_d	if $k_t<k_t\ max$, $f_d>f_d\ min$	$k_t\ max$= 0.20, $f_d\ min$ = 0.90	2.7
F5	upper limit for f_d	for z < 75° , $f_d<f_d\ max1$ for z ≥ 75° , $f_d<f_d\ max2$	$f_d\ max1$ = 1.05 $f_d\ max2$ = 1.10	0.8
F6	limits on k_{tp}	$0 <k_{tp}<k_{tp}\ max$	$k_{tp}\ max$ = 1.35	0.0
F7	limits on f_p	f_p min $<f_p<f_p\ max$	$f_p\ min$ = 1.7 μmol/J $f_p\ max$ = 10 μmol/J	0.4
F8	limits on Q_p	$\alpha_{min}k_t < Q_p < \alpha_{max}k_t$	α_{min} = 340 μmol/m^{2}s α_{max} = 4000 μmol/m^{2}s	1.5
ALL	all filters	all the above conditions		4.9

It has been observed (Foyo-Moreno et al., 2017) that PAR flux data Q_p can be bounded by two straight lines in a Q_p vs k_t diagram. This can be understood since the PAR photon flux is highly correlated with global horizontal irradiance GHI, as shown in Fig. 1 (a). If a linear relationship is assumed, $Q_p = a \times GHI = \alpha \times k_t$, with slope of $\alpha \approx a \times G_0\ /m$, in terms of the relative air mass (Kasten and Young, 1989). The extreme values for these slopes are associated to the extreme values of air mass in the data (between 1 and 8.21), to the 3% variation in G_0 due to the orbital factor and to the natural dispersion in the (Q_p, G_h) diagram. The estimated value of a, obtained by simple regression through the origin, is $a = 2.1 \pm 0.2$ μmol/J (similar to the average PAR fraction). Taking into account these variations, extreme values of α can be estimated as $\alpha_{min} \approx 340$ μmol/m^{2}s and $\alpha_{max} \approx 2900$ μmol/m^{2}s.

As shown in Fig. 1 (b), the lower limit follows this slope quite well. The calculated upper limit (associated to mostly clear-sky samples) shows to over-filter portions of the data cloud, especially at low k_t values. Therefore, this slope in filter F8 has been increased in order to preserve valid data points for low k_t values. Filter F8 restricts valid Q_p data to lie between two lines through the origin with slopes of $\alpha_{min} = 340$ μmol/m^{2}s and $\alpha_{max} = 4000$ μmol/m^{2}s, as shown in Fig. 1 (b). Less than 5% of the baseline records are discarded by this procedure (Table 2) resulting in 791161 records with valid (G_h, Q_p) pairs.

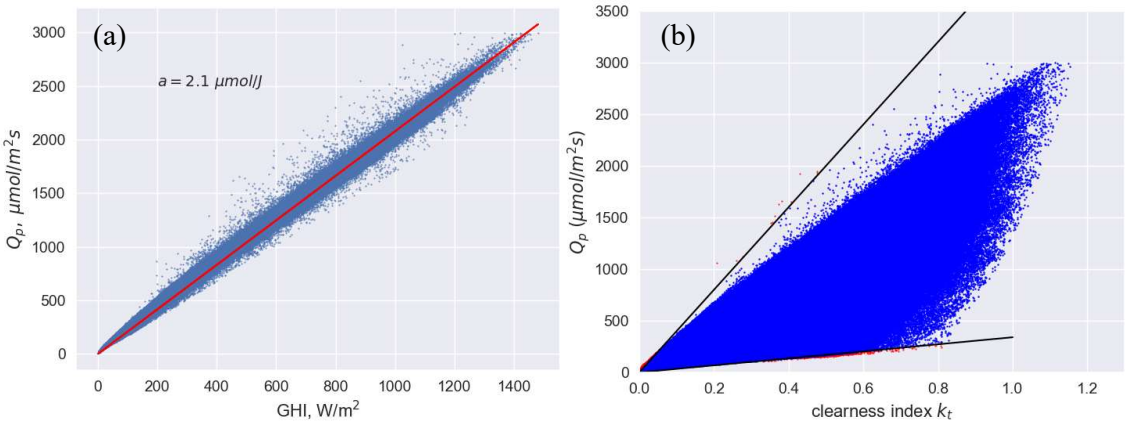

Figure 1: Left: Correlation between *Qp* and *Gh*; the red line results from a linear regression through the origin (intercept equal to zero). Right: Effect of filter F8 in the *Qp* and *kt* space.

The resulting PAR fraction vs clearness index scatter-plot is shown in Fig. 2. Under heavy cloud cover ($k_t < 0.20$) the PAR fraction increases sharply due to the enhanced infrared absorption and the predominance of diffuse irradiance (Iqbal, 1983). On the other hand, for $k_t > 0.20$, $f_p \approx 2$ μmol/J with weak dependence on *kt*.

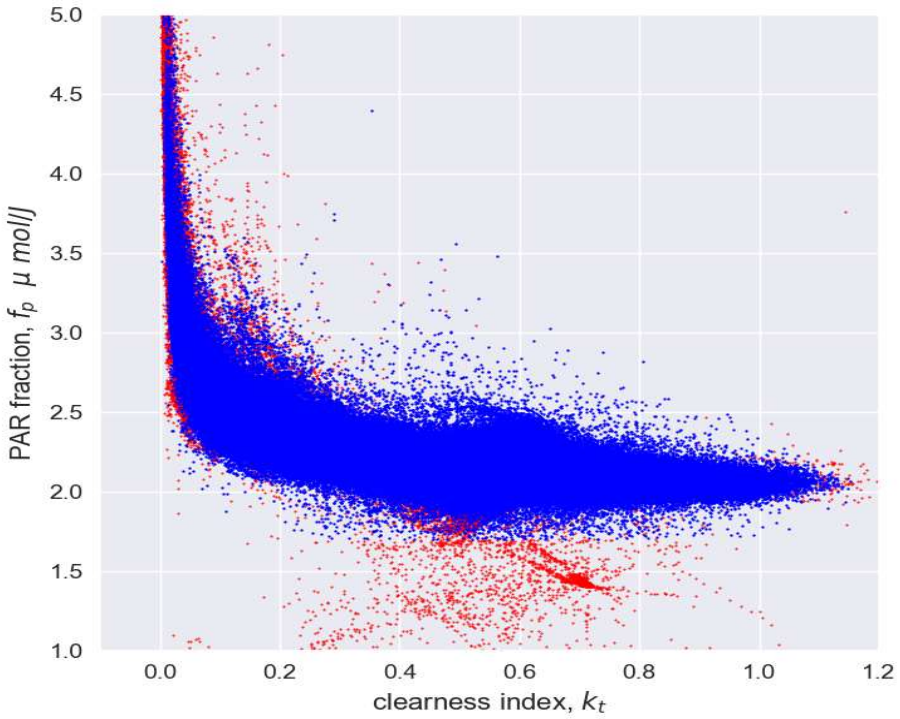

Figure 2: PAR fraction vs clearness index after all filters in Table 1 have been applied. The discarded data points are shown in red.

2.2 Models and methodology

As mentioned in the introduction, the pre-existing PAR fraction models considered in this work are those listed in Table 1. All these models are originally based on hourly aggregated data and use the clearness index k_t and the sine of the solar altitude (or, equivalently *cos(z)*) as independent predictor variables. In Eqs. (1) to (4) below, the parametric form for each of these models are provided,

AL $f_p = a + b\ ln(k_t) + c\ sin\alpha_s$ (1)

TL $f_p = a\ (sin\ \alpha_s)^b$ (2)

ES $f_p = a + bk_t + ck_t^2 + dk_t^3$ (3)

TW $f_p = a + bk_t + ck_t^2$ (4)

where a, b, c and d are coefficients (in μmol/J, except for b in Eq. (2) which is dimensionless) that can be adjusted to local data. The original values of these coefficients are listed in Table 3. These models are supplemented by the constant value f_p = 2.096 μmol/J previously found from data for the Pampa Húmeda region by Grossi-Gallegos et al. (2004). Almost all models use the clearness index k_t and two of them (AL and TW) include a dependence on the relative air mass through the solar altitude angle.

The performance of these models is evaluated with their original coefficients and when the coefficients are adjusted to the local data using a standard multivariable linear regression technique. In the case of Eq. (2), the dependence on the parameter b is not linear, but it can be linearized by taking the natural logarithm of both sides.

The evaluation of the original models is done against the filtered data set. The training and evaluation of local models is done by using a standard random sampling and cross-validation method in which, at each iteration, 50% of the data is used for adjustment and the other 50% is used for testing. After 1000 iterations, the average values are used for the local parameters and for the performance indicators.

The evaluation of the models is done by calculating the residuals, $\xi = \widehat{f_p} - f_p$, between the estimated PAR fraction, $\widehat{f_p}$, and the corresponding measurement f_p. The mean bias deviation (MBD), the mean absolute deviation (MAD) and the root mean squared deviation (RMSD) metrics are used for the comparison,

$$MBD = \frac{1}{N}\sum_{i=1}^{N}\xi_i, \quad MAD = \frac{1}{N}\sum_{i=1}^{N}|\xi_i| \quad \text{and} \quad \text{RMSD} = \sqrt{\frac{1}{N}\sum_{i=1}^{N}\xi_i^2}, \tag{5}$$

expressed in relative terms as a percentage of the measured PAR fraction average of 2.191 μmol/J. The integer quantity N = 791161 is the number of valid 1-min data records, resulting from the quality control procedure described in Subsection 2.1

A comparison with the original performance of some of the models is not straightforward. In some cases, these metrics are not reported. In others, it is unclear if an independent data set is used for evaluation and training. For the AL and TW PAR fraction models, independent datasets for training and evaluation are used and the absolute MBD and RMSD indicators for the derived PAR irradiance (in W/m^2) are reported, but the corresponding mean PAR irradiance is not given. In order to compare with these cases, the horizontal PAR irradiance is calculated as $G_p = Q_p/\kappa = f_p \times G_h/\kappa$ with κ = 4.566 μmol/J and, after expressing our

relative indicators for f_p in absolute terms, obtain the desired performance indicators for the derived quantity, G_p .

3. Results and discussion

The previously presented models were proposed and adjusted by their authors for the hourly time scale, so they are not expected to perform as well with 1-minute data, which has significantly higher variability. This kind of comparison has been done before with diffuse fraction models (Engerer, 2015; Gueymard and Ruiz-Arias, 2016), investigating at which extent hourly models still hold or underperform when 1-min data is used. The result, of course, depends on the model.

Table 3 lists the original and locally adjusted coefficients for each model. The adjustments and performance of the original models is not only affected by the time scale of the data, but also by the typical local climate of the site and the characteristics of the data being used, so the original vs local parameter comparison is not straightforward. As a sanity check, it is noted that the sign of the parameters do not vary when locally adjusted and changes in their value are small, with the exception of the higher order terms of the ES model and the term associated with the solar altitude of the AL model.

Table 3: Original and adjusted coefficients for the PAR fraction models. Coefficient *b* in the TL model is dimensionless.

Model	Parameters	a (µmol/J)	b (µmol/J)	c (µmol/J)	d (µmol/J)
AL	original	1.83	-0.19	0.10	--
AL	locally adjusted	2.01	-0.26	-0.03	--
TL	original	1.99	-0.07	--	--
TL	locally adjusted	2.13	-0.04	--	--
ES	original	2.73	-2.39	3.46	-1.56
ES	locally adjusted	3.04	-4.83	8.29	-4.70
TW	original	2.82	-1.54	0.56	--
TW	locally adjusted	2.79	-2.07	1.48	--
constant	Grossi et al. 2004	2.10	--	--	--
constant	locally adjusted	2.19	--	--	--

Table 4 presents the performance evaluation of the models with their original coefficients, including as a baseline the constant value f_p = 0.4604 × 4.566 µmol/J = 2.10 µmol/J (last row), obtained by Grossi Gallegos et al. (2004) for San Miguel, Argentina, a site located about 370 km from the LES site used for this work. The local version is the average PAR fraction obtained from our filtered dataset. They differ in about 4%, which is similar to the uncertainty in the data. The relevant performance metrics for each model (both original and locally adjusted) are given in Table 4. As expected, the constant models are among the worst in terms of RMSD.

When the original models are considered, all of them fall in a narrow range: relative MBDs between 4 and 7 % and RMSDs between 8 and 11%. The hourly-adjusted polynomial

models TW and ES (Tsubo and Walker, 2007; Escobedo et al., 2006) with their original coefficients provide the best local performance for 1-minute data, showing the lowest bias and dispersion. The second order polynomial of Tsubo and Walker performs slightly better, probably due to a higher robustness (polynomial instability increases with its order, specially for extrapolations). The original Alados et al. model comes third in performance, quite close to the first two in terms of rRMSD, but with higher bias (indeed, the worst bias). The Tiba and Leal model with original coefficients does not improve on the utilization of a constant value for the PAR fraction, nor in bias or dispersion. The polynomial models of Eqs. (3) and (4) with their original coefficients are the ones which better represent the local data and, therefore, are the recommended original models for the region.

Table 4 also presents the performance of the models with local adjustment. When the models are locally fitted, the analysis changes. The range of RMSDs is now between 5 to 10%, with negligible biases and all local models outperform the local constant value, as expected (they include extra variables with some predictive power). However, it observed that the Tiba and Leal model only improves the constant value to a small extent, hence the solar altitude as the single input variable seems to be inadequate for this problem. The models that use k_t as input show the higher improvements with respect to the local constant value. The locally adjusted model AL based on *log* (k_t) is the best local model, followed by the polynomial k_t models ES and TW.

Table 4: Performance evaluation of the original models. The average for the relative metrics is 2.191µmol/J.

Model	Parameters	rMBD (%)	rMAD (%)	rRMSD (%)
AL	original	-6.9	7.0	9.2
AL	locally adjusted	0.0	3.3	5.4
TL	original	-5.3	6.5	11.5
TL	locally adjusted	-0.2	6.1	10.2
ES	original	3.8	6.0	8.0
ES	locally adjusted	0.0	3.3	5.6
TW	original	-0.8	6.0	7.9
TW	locally adjusted	0.0	3.8	6.3
constant	original	-3.3	6.0	10.9
constant	local	0.0	6.5	10.4

Figure 3 shows the dataset for PAR fraction vs k_t with the estimates from the original (violet) and the locally adjusted (red) models superposed. The PAR fraction at a 1 minute rate has an important enhancement for lower k_t values (cloudy conditions) and some locally adjusted models are not able to capture this feature in spite of their good performance metrics.

As Fig. 3c and 3e show (TW and ES models), the locally adjusted polynomial models are unable to adequately represent the variability of the 1-minute PAR fraction data, having acceptable overall metrics at the cost of misrepresenting data for either low or high k_t values. In particular, important deviations are observed for high k_t values (clear sky) in both polynomial models. On the other hand, the locally adjusted AL model (Fig. 1b) adequately

represents the PAR fraction tendency over the whole range of k_t. Finally, it is also observed that the constant value and the TL model are not able to reproduce the PAR fraction enhancement under cloudy skies, and this fact explains their poor performance indicators.

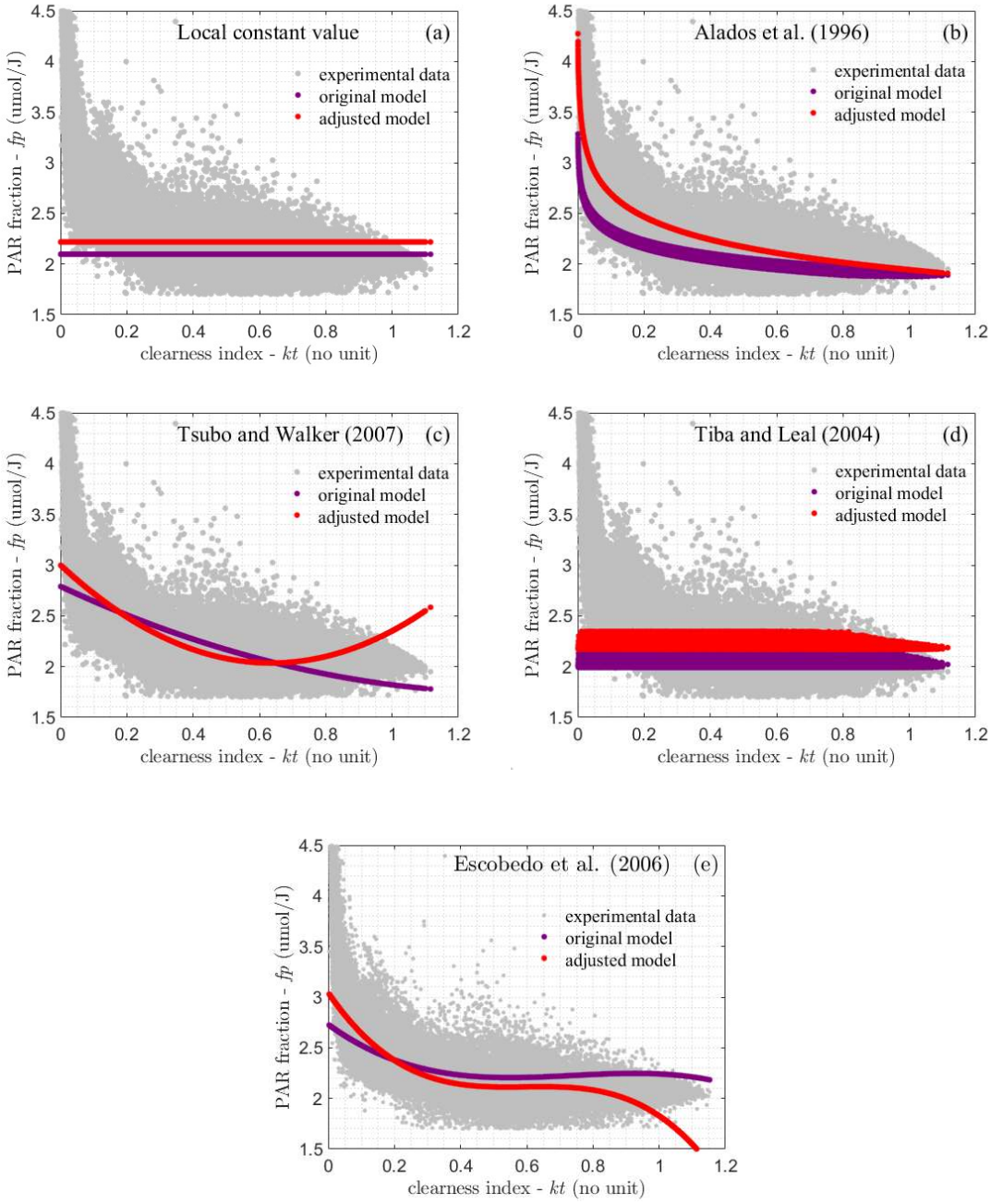

Figure 3: PAR fraction as a function of kt (1-minute time basis). Filtered data is shown as gray dots. The original model predictions are in red and the local adjusted model's predictions are shown in violet.

4. Conclusions

A first assessment of PAR fraction models in Uruguay has been presented. Four pre-existing empirical models, developed originally for the hourly timescale, were implemented and evaluated, in their original and locally adapted versions using a 1-minute quality-controlled dataset with four years of PAR photon flux and GHI data for a single location, representative of the Pampa Húmeda region of south-east South America. The frequently used constant

value for PAR fraction has also been tested, as a baseline model. The conclusions of this work are summarized as follows:

- The average PAR fraction *fp* was found to be 2.19 μmol/J, which is only 4% above the previous value obtained for this region using indirect pyranometer-based measurements (Grossi-Gallegos et al. 2004).
- The hourly adjusted polynomial models of Escobedo et al. (2006) and Tsubo and Walker (2005) with their original coefficients represent reasonably well the local 1-minute PAR fraction data with mean biases which are -1% to 4% of mean f_p.
- Overall metrics are improved significantly by the local adaptation. In spite of this, for the TW and ES models, the local adjustment with 1-minute data is not able to represent the PAR fraction behavior for the whole range of clearness index. For this reason, their use in the region is not recommended at the 1 minute timescale. We tested higher degree polynomials (up to eight degree) and none of them was able to adequately represent the 1-minute PAR fraction behavior.
- The solar altitude as input variable provides marginal gains. The TL model, which uses only this variable, has no significant advantage over the constant model for 1-minute PAR fraction data.
- The best locally adjusted model was the one proposed in Alados et al. (1996). This model has a logarithmic dependence on the clearness index which adequately represents the 1-minute f_p behavior, especially its enhancement under overcast conditions. This was the best performing local model at the 1-minute time scale with RMSD of around 5% and negligible bias.

5. References

Abal, G., Aicardi, D., Alonso Suárez, R., Laguarda, A., 2017. Performance of empirical models for diffuse fraction in Uruguay. Solar Energy 141, 166-181. DOI: 10.1016/j.solener.2016.11.030.

Abal, G., Monetta, A., Alonso-Suárez, R., 2018. Outdoor solar radiometer calibration under ISO 9847:1992 standard and alternative methods. Proceedings of the IEEE 9th Power, Instrumentation and Measurement Meeting (EPIM), pp. 1-6. DOI: 10.1109/EPIM.2018.8756376.

Alados, I., Foyo-Moreno, I., Alados-Arboledas, L., 1996. Photosynthetically active radiation: measurements and modelling. Agricultural and Forest Meteorology 78, 121-131. DOI: 10.1016/0168-1923(95)02245-7.

Alonso-Suárez, R., Abal, G., Siri, R., Muse, P., 2014. Satellite-derived solar irradiation map for Uruguay. Energy Procedia 57, 1237-1246. DOI: 10.1016/j.egypro.2014.10.072.

Engerer, N.A., 2015. Minute resolution estimates of the diffuse fraction of global irradiance for southeastern Australia. Solar Energy 116, 215-237. DOI: 10.1016/j.solener.2015.04.012.

Escobedo, J.F., Gomes, E., de Oliveira, A., Soares, J., 2006. Radiações Solares UV, PAR e IV: Estimativa em funcão da Global. Avances en Energías Renovables y Medio Ambiente (AVERMA) Vol. 10, 11-79-11-86.

Foyo-Moreno, I., Alados, I., Alados-Arboledas, L., 2017. A new conventional regression

model to estimate hourly photosynthetic photon flux density under all sky conditions. Int. J. Climatol. 37, 1067-1075. DOI: 10.1002/joc.5063.

Grossi Gallegos, H., Righini, R., Dursi, O., 2004. Primeras Mediciones de la Radiación Fotosintéticamente Activa en San Miguel, Provincia de Buenos Aires Avances en Energías Renovables y Medio Ambiente (AVERMA) Vol. 8, 11.13-11.17.

Gueymard, C.A., Ruiz-Arias, J.A., 2016. Extensive worldwide validation and climate sensitivity analysis of direct irradiance predictions from 1-min global irradiance, Solar Energy 128, 1-30. DOI: 10.1016/j.solener.2015.10.010.

Iqbal, M., An Introduction to Solar Radiation. Academic Press, Toronto, 1983.

Kasten, F.,Young, A.T., 1989. Revised optical air mass tables and approximation formula. Applied optics 28, 4735-4738. DOI: 10.1364/AO.28.004735.

Kopp, G., Lean, J., 2011. A new, lower value of total solar irradiance: evidence and climate significance. *Geophys. Res. Lett.*, 38, L01706. DOI: 10.1029/2010GL045777.

Long C.N., Shi Y. 2006. The QCRad value added product: surface radiation measurement quality control testing, including climatologically configurable limits. Atmospheric Radiation Measurement Program, Technical Report, ARM TR-074. Available at https://www.arm.gov/publications/tech_reports/doe-sc-arm-tr-074.pdf.

Peel, M. C., Finlayson, B. L., Mcmahon, T. A., 2007. Updated world map of the Köppen-Geiger climate classification. Hydrology and Earth System Sciences Discussions 11:1633–1644. DOI: 10.5194/hess-11-1633-2007.

Perez, R., Inechien, P., Seals, R.,Zelenka, A., 1990. Making full use of the clearness index for parameterizing hourly insolation conditions. Solar Energy 45, 111-114. DOI: 10.1016/0038-092X(90)90036-C.

Tiba, C., Leal, S., 2004. Medidas e modelagem da radiação PAR para o nordeste do Brasil. 5º Encontro de Energia no Meio Rural e Geração Distribuída, pps. 1-8, Campinas, São Paulo.

Tsubo, M., Walker. S., 2005. Relationships between photosynthetically active radiation and clearness index at Bloemfontein, South Africa. Theor. Appl. Climatol. 80, 17-25. DOI: 10.1007/s00704-004-0080-5.